2013 European Control Conference (ECC)
July 17-19, 2013, Zürich, Switzerland.

State Estimation with Time Delay and State Feedback Control of Cathode Exhaust Gas Mass Flow for PEM Fuel Cell Systems

Martin Schultze and Joachim Horn
Institute of Control Engineering, Helmut-Schmidt-University Hamburg

Abstract— **Polymer electrolyte membrane (PEM) fuel cells are highly efficient energy converters and provide electrical energy, cathode exhaust gas with low oxygen content and water. On aircraft fuel cells have the potential of replacing the auxiliary power unit (APU) that is currently used for electrical power generation during ground operations. An APU is a significant source of noise and greenhouse gases. PEM fuel cells, however, can significantly reduce these pollutants.**

In this study a PEM fuel cell system is investigated for generation of oxygen depleted cathode exhaust air (ODA). This gas is intended for inerting on aircraft and must have a low oxygen concentration. A nonlinear simulation model comprising the fuel cell stack, stack cooling system and cathode exhaust gas dehumidifying system has been developed and a reduced order model for controlling ODA-gas mass flow was derived. An observer for state estimation combined with a predictor to compensate for the large time delay occurring has been designed. ODA mass flow is controlled for by a linear state feedback controller. Simulation results performed at the nonlinear simulation model in Matlab/Simulink® and experimental results are shown.

I. Introduction

Generation of oxygen depleted cathode exhaust air (ODA) for tank inerting on aircraft [1] is a central aspect of the multifunctional use of a PEM fuel cell system. For this application oxygen concentration in ODA-gas must be close to or less than 10% (vol.) [2]. On aircraft auxiliary power units (APU) provide electrical power during ground operations. However, these APUs are significant sources of greenhouse gases such as CO_2 and NO_x as well as noise. PEM fuel cells are very efficient energy converters and have the potential of significantly reducing emission of these pollutants. Among other types of fuel cells they are the most suitable for dynamic applications and hence studied for replacing APUs. PEM fuel cell systems have been studied for electrical power supply of autonomous robots [3] or for automotive applications [4, 5]. Operation of PEM fuel cell systems for inerting has not yet been studied in detail.

Proper fuel cell system operation such as keeping the polymer membrane well hydrated as well as proper supply of fuel and air as oxygen carrier is a central aspect [6]. The fuel cell system used in this study has an anode recirculation loop for an efficient use of hydrogen fuel and for gas as well as membrane humidification. A water separator installed in the recirculation loop prevents anode flooding, which is more likely to occur than cathode flooding [7] as cathode gas flow continuously removes cathode water. Fuel and air supply as well as temperature gradient across the stack is managed by an internal fuel cell system controller. The fuel cell stack is connected to a controllable ohmic load that draws a stack current as requested.

Figure 1 shows a schematic of the multifunctional fuel cell system (MFFCS) with ODA gas conditioning in the cathode exhaust gas line. Depending on stack temperature product water partly evaporates and leaves the stack as water vapor, whereas the remaining liquid leaves the cathode as liquid water, which is mostly separated by the upstream water separator (Sep. 1). In a condenser the vapor is cooled and condenses into liquid water, which is separated in the downstream water separator (Sep. 2). Oxygen excess ratio, which is termed stoichiometry (stoic) as well as stack current (I_{stack}), stack and condenser cooling inlet temperatures ($T_{stackin}$ and T_{condin}) are fuel cell system input parameters. The fuel cell system model is based on the model reported of in [8] and is augmented by two water separators, connecting volumes and a stationary condenser model as in [9]. The simulation model is briefly outlined in section II. fuel cell system model. Control strategy with state-feedback controller, observer and predictor is described in section III. ODA mass flow control.

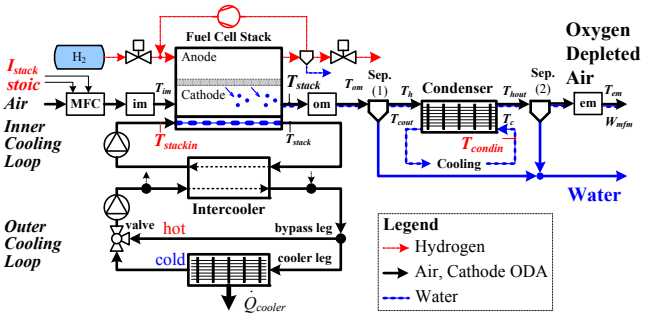

Fig 1. Schematic of the fuel cell system comprising stack, up- and downstream water separators (Sep.1, 2), condenser and connecting volumes: inlet-, outlet- and exit manifold (im, om, em); Hydrogen is recirculated and water is removed in an anode water separator; stack and condenser are cooled by separate cooling systems

II. Fuel Cell System Model

The fuel cell system model comprises the fuel cell stack, a mass flow controller (MFC) for cathode feed air supply and

This study as part of the project "cabin technology and multifunctional fuel cell systems" has been supported by Airbus and the German Federal Ministry of Education and Research (support code: 03CL03A).

Martin Schultze and Joachim Horn are with the Institute of Control Engineering, Helmut-Schmidt-University Hamburg, Holstenhofweg 85, D-22043 Hamburg, Germany (e-mail: Martin.Schultze@hsu-hh.de, Joachim.Horn@hsu-hh.de).

an anode hydrogen recirculation. The MFC delivers an air mass flow as specified by stoichiometry and stack current. The internal controller operates the stack cooling pump to set the reference temperature difference across the fuel cell stack. Inlet air is modeled as a dry and ideal gas consisting of 21% (vol.) oxygen and 79% (vol.) nitrogen. A list of the model parameters is given in table 1 at the end of this paper.

A. Cathode and Anode Model

A lumped volume with homogeneous temperature is assumed for the cathode, whose temperature is assumed to be stack temperature. The model is derived from first principles with mass conservation (1) for oxygen and nitrogen [4, 8]. Gases are assumed ideal and their partial pressures are determined by the ideal gas law (1).

$$(1)\quad \frac{dm_{O2}}{dt} = W_{im,O2} - W_{O2rct} - W_{ca,O2},\quad p_{O2} = m_{O2}\frac{T_{stack}R_{O2}}{V_{ca}}$$
$$\frac{dm_{N2}}{dt} = W_{im,N2} - W_{ca,N2},\quad p_{N2} = m_{N2}\frac{T_{stack}R_{N2}}{V_{ca}}$$

Condensation is assumed to occur instantaneously and water is transported out of the cathode as vapor and liquid. Water also diffuses through the membrane to the anode. The membrane model is given in [4, 8]. To prevent anode flooding a water separator removes water from the hydrogen gas flow in the anode recirculation loop, in which a compressor recirculates hydrogen gas. As proposed by [5] the anode model has been extended for anode water removal (2) with separation efficiency $\eta_{sep,an}$ and the hydrogen compressor maximum mass flow $W_{recirc,max}$ with $m_{H2O,an}$ being the mass of water and $m_{H2,an}$ the mass of hydrogen in the anode and membrane water flow W_{mem}(3).

$$(2)\quad W_{sep,an} = \eta_{sep,an} W_{recirc,\max}\frac{m_{H2O,an}}{m_{H2O,an} + m_{H2,an}}$$

$$(3)\quad \frac{dm_{H2O,an}}{dt} = -W_{mem} - W_{sep,an}$$

Recirculation pump speed increases with stack current. The higher the hydrogen mass flow in the recirculation line, the more water is separated. An empirical approach (4) with parameters k_1 and k_2 has been chosen to describe the separation efficiency in terms of stack current.

$$(4)\quad \eta_{sep,an} = \exp(k_1 + k_2 I_{stack})$$

B. Stack Thermal Model

Fuel cell stack temperature T_{stack} is obtained by energy conservation (5) with stack heat capacity C_{stack}. The energy flows are given by chemical energy provided by hydrogen (higher heating value of H_2 leading to a virtual cell voltage of 1.48V), electrical energy delivered by the stack and thermal energy flows of ODA-gas, liquid water, water vapor and anode water separation mass flow $W_{sep,an}$. Energy conservation (5) is obtained using stack cooling inlet temperature $T_{stackin}$, cooling mass flow W_{int}, feed air mass flow W_{im} from inlet manifold with temperature T_{im}, ODA mass flow $W_{ca,oda}$ and $W_{ca,odacell} = W_{ca,oda}/n_{cells}$ as the ODA mass flow per cell, liquid $W_{ca,l}$ and vapor mass flow $W_{ca,v}$ leaving the stack. The specific heat capacities are c_{cool}, c_{air}, c_{oda}, c_l, c_v and h_0 being the enthalpy of evaporation of water. The number of cells in the fuel cell stack is n_{cells}.

$$(5)\quad \begin{aligned} C_{stack}\frac{dT_{stack}}{dt} &= (1.48\, n_{cells} - U_{stack})I_{stack} + W_{cool}c_{cool}(T_{stackin} - T_{stack}) \\ &\quad + W_{im}c_{air}(T_{im} - T_0) - W_{ca,oda}c_{oda}(T_{stack} - T_0) \\ &\quad - W_{ca,l}c_l(T_{stack} - T_0) - W_{ca,v}(h_0 + c_v(T_{stack} - T_0)) \\ &\quad - W_{sep,an}c_l(T_{stack} - T_0) \end{aligned}$$

C. Outlet- and Exit Manifold Model

Compared to [8] the fuel cell system model is extended by an exit manifold model. The cathode exhaust gas cools down in the outlet manifold. Outlet manifold temperature T_{om} is lower than stack temperature, which is accounted for by a constant temperature loss $T_{om} = T_{stack} - T_{om,loss}$. As compared to [8] the water dynamics of the outlet and exit manifold are approximated by a static behavior. This is reasonable as it is not measurable how much liquid water resides in the manifolds. ODA-gas still has a temperature of 50-70°C in the outlet manifold. Simply neglecting the vapor or liquid water mass flows would be inaccurate. However, as enough liquid water is carried by the gas stream, a relative humidity of 100% is assumed. So, the vapor pressure can be considered saturation vapor pressure p_v^{sat} [8, 10]. Outlet manifold vapor mass flow $W_{om,v}$ is determined by water loading X_{om}. Vapor mass flow cannot exceed the vapor and liquid inlet mass flow from cathode $W_{ca,v}$ and $W_{ca,l}$. This is accounted for by taking the minimum of inlet and maximum possible mass flow. The remainder is liquid water $W_{om,l}$ (6). Water loading is $X_{om} = p_v^{sat}/(p_{om}-p_v^{sat})*R_{oda}/R_v$ with vapor gas constant R_v and the ODA gas constant R_{oda} being approximated by air. A turbulent flow establishes at the outlet manifold exit and is modeled as (7) with the flow constant c_{sep1} and the pressure gradient of outlet manifold p_{om} and condenser inlet pressure $p_{cond,in}$. Outlet manifold pressure is obtained by $p_{om} = p_v^{sat} + p_{om,oda}$.

$$(6)\quad \begin{aligned} W_{om,v} &= \min(X_{om}W_{om,oda}, W_{ca,v} + W_{ca,l}) \\ W_{om,l} &= W_{ca,v} + W_{ca,l} - W_{om,v} \end{aligned}$$

$$(7)\quad W_{om} = c_{sep1}\sqrt{(p_{om} - p_{cond,in})}$$

$$(8)\quad \frac{dm_{om,oda}}{dt} = W_{ca,oda} - \frac{1}{1 + X_{om}}W_{om},\quad p_{om,oda} = m_{om,oda}\frac{T_{om}R_{oda}}{V_{om}}$$

The same applies for the turbulent flow W_{em} in the exit manifold. The flow is modeled according to (7) with flow constant c_{em} and pressure difference of exit manifold and ambient ($p_{em} - p_{amb}$). Fluid flow into the exit manifold is modeled as turbulent assuming that vapor mass flow is small compared to ODA mass flow through the downstream separator. So, ODA mass flow $W_{sep2,oda}$ into the exit manifold is gained by (9) with constant c_{sep2} and pressure difference of condenser outlet $p_{cond,out}$ and p_{em}.

$$(9)\quad W_{sep2,oda} = c_{sep2}\sqrt{(p_{cond,out} - p_{em})}$$

The ratio of water to dry ODA mass flow is termed ODA water loading X_{oda} and has units of g/kg. It is gained as the ratio of the sum of vapor $W_{em,v}$ and liquid $W_{em,l}$ mass flow to dry ODA mass flow $W_{em,oda}$ in the exit manifold (10).

(10) $X_{oda} = \left(W_{em,v} + W_{em,l}\right)/\left(W_{em,oda}\right) \times 1000$

The humid ODA-gas mass flow is measured by a mass flow meter installed at a distance after the condenser. Due to the pipe length a significant transport delay T_d is introduced. In order to measure water loading, ODA-gas is heated up from T_{em} to T_{mfm} along the pipe such that remaining liquid water carried evaporates. The pressure is $p_{mfm} = p_{em}$. A static model with $X_{mfm}=X_{oda}$ given in the following describes this behavior. Value RH (11) is obtained by the ideal gas law.

(11) $RH = \left(p_{mfm} R_v X_{mfm}\right)/\left(p_v^{sat}(T_{mfm})\left(R_{oda} + X_{mfm} R_v\right)\right)$

For $RH < 1$ relative humidity measurement is $\phi_{\mathrm{mfm}}=RH$, vapor mass flow $W_{mfm,v}=W_{em,v}+W_{em,l}$ and of liquid $W_{mfm,l}=0$. For $RH \geq 1$ the mass flows are governed with $\phi_{\mathrm{mfm}}=1$, $W_{v,mfm} = \frac{p_v^{sat}(T_{mfm})}{p_{mfm} - p_v^{sat}(T_{mfm})} \frac{R_{oda}}{R_v} W_{em,oda}$ and $W_{mfm,l}=(W_{em,v}+W_{em,l})-W_{mfm,v}$. The mass flow meter is modeled to measure ODA-gas and vapor mass flow with constant time delay T_d as follows (12).

(12) $W_{mfm}(t) = W_{em,oda}(t - T_d) + W_{mfm,v}(t - T_d)$

D. Water Separator Model

Up- and downstream cyclone water separators (Sep. 1, 2) are modeled equivalently. Their pressure loss is low, such that condensation or evaporation inside the separators can be neglected. The separation efficiency $\eta_{separator}=100\%$ is assumed constant. Both are implemented as static models. Equations for the separator are (13). A water mass flow of W_{sepUp} is removed by the upstream separator. Liquid and vapor mass flows from the condenser outlet enter the downstream separator, where W_{sepDn} is removed.

(13)
$$\begin{aligned} W_{sep1,v} &= W_{om,v} \\ W_{sep1,l} &= \left(1 - \eta_{separator}\right) \cdot W_{om,l} \\ W_{sepUp} &= \eta_{separator} \cdot W_{om,l} \end{aligned} \quad \text{and} \quad \begin{aligned} W_{sep2,v} &= W_{cond,v} \\ W_{sep2,l} &= \left(1 - \eta_{separator}\right) \cdot W_{cond,l} \\ W_{sepDn} &= \eta_{separator} \cdot W_{cond,l} \end{aligned}$$

E. Voltage Model

Stack voltage $U_{stack} = n_{cells} U_{cell}$ is the sum of all n_{cells} cell voltages. Cell voltage is modeled as $U_{cell} = U_{rev} - \eta_{act} - \eta_{\Omega}$ (14) with the reversible cell voltage U_{rev}, activation loss η_{act} [11] and ohmic loss η_{Ω} [12]. The membrane thickness is given by d_m and the active surface area by A_{sfc}. Parameters $\zeta_1,\ldots\zeta_4$ and $b_1,\ldots b_3$ have been identified by a least square error minimization using experimental data as shown in [8].

(14)
$$\begin{aligned} U_{rev} &= 1.229 - 0.85 \cdot 10^{-3}\left(T_{stack} - 298.15\right) + 4.3 \cdot 10^{-5} T_{stack}\left(\ln \tfrac{p_{H2}}{p_0} + \tfrac{1}{2} \ln \tfrac{p_{O2}}{p_0}\right) \\ \eta_{act} &= \zeta_1 + \zeta_2 T_{stack} + \zeta_3 T_{stack} \ln\left(p_{O2} e^{(498/T_{stack})} / 5.08 \cdot 10^{-6}\right) + \zeta_4 T_{stack} \ln\left(I_{stack}\right) \\ \eta_{\Omega} &= \frac{d_m}{\left(b_1 \lambda_m - b_2\right)} e^{-b_3\left(\frac{1}{303} - \frac{1}{T_{stack}}\right)} \frac{I_{stack}}{A_{sfc}} \end{aligned}$$

F. Condenser Model

The condenser model is derived from a differential and stationary model of a counter flow condenser as shown in figure 2. The model is based on the effectiveness-NTU method [13] with NTU being the number of transfer units, which is an important parameter in heat exchanger modeling. The model is compared to a 50 cell condenser model in [9] and shows good results. The heat transfer coefficient of a differential element is U. ODA-gas is assumed to enter and leave the condenser fully saturated. It is fully saturated inside the condenser. ODA-gas, vapor and liquid are assumed to exhibit equal temperature.

Vapor condenses as it travels through the condenser leading to a flow resistance increase. Condenser flow is turbulent and is modeled as an ODA and vapor mass flow. As the vapor mass flow is assumed not to change across the upstream water separator, the condenser inlet vapor mass flow is modeled as $W_{om,v}=X_{om}W_{cond,oda}$. ODA mass flow through the condenser is obtained by (15) resulting in an ODA-gas mass flow through the separators and the condenser (16) governed by equations (7), (9) and (14).

(15) $\left(1 + X_{OM}\right)^2 W_{cond,oda}{}^2 = c_{cond}{}^2 \left(p_{cond,in} - p_{cond,out}\right)$

(16) $W_{cond,oda} = \sqrt{p_{om} - p_{em}} \Bigg/ \sqrt{\frac{\left(1 + X_{om}\right)^2}{c_{sep1}{}^2} + \frac{\left(1 + X_{om}\right)^2}{c_{cond}{}^2} + \frac{1}{c_{sep2}{}^2}}$

Temperature gradient driven heat transfer from ODA to cooling side and neglecting higher order terms leads to (17). Energy balance (18) across a cooling cell and applying a Taylor series expansion and neglecting higher order terms leads to (19).

(17) $\dot{Q}(z) = U dz \left(T_h(z) - T_c(z)\right)$

(18) $0 = W_{cool} c_c T_c(z + dz) - W_{cool} c_c T_c(z) + \dot{Q}(z)$

(19) $W_{cool} c_c \frac{\partial T_c}{\partial z} = C_c \frac{\partial T_c}{\partial z} = -U\left(T_h(z) - T_c(z)\right)$

ODA mass flow is assumed constant and a mean pressure p_c governed by the arithmetic mean of condenser inlet and outlet pressure (20) is assumed as condenser pressure. Water loading of fully saturated ODA is modeled as (21) using the temperature of ODA $T_h(z)$. Energy balance at the ODA side is (22). Applying a Taylor series expansion and neglecting higher order terms reduces (22) further leading to (23).

(20) $p_c = \tfrac{1}{2}\left(p_{cond,in} + p_{cond,out}\right)$

(21) $X(z) = \frac{p_v^{sat}(T_h(z))}{p_c - p_v^{sat}(T_h(z))} \frac{R_{oda}}{R_v}$

(22)
$$\begin{aligned} 0 = {} & W_{cond,oda} c_{oda} T_h(z) + W_v(z)\left(h_0 + c_v T_h(z)\right) + W_l(z) c_l T_h(z) \\ & - W_{cond,oda} c_{oda} T_h(z + dz) - W_v(z + dz)\left(h_0 - c_v T_h(z + dz)\right) \\ & - W_l(z + dz) c_l T_h(z + dz) - U dz \left(T_h(z) - T_c(z)\right) \end{aligned}$$

(23)
$$\begin{aligned} 0 = {} & -W_{cond,oda} c_{oda} \frac{\partial T_h}{\partial z} dz - h_0 \frac{\partial W_v}{\partial z} dz - U dz \left(T_h(z) - T_c(z)\right) \\ & - c_v \left(W_v(z) \frac{\partial T_h}{\partial z} dz + \frac{\partial W_v}{\partial z} T_h(z) dz\right) \\ & - c_l \left(W_l(z) \frac{\partial T_h}{\partial z} dz + \frac{\partial W_l}{\partial z} T_h(z) dz\right) \end{aligned}$$

Differentiation of $W_v(z) = X(z) W_{cond,oda}$ with respect to z leads to $\frac{\partial W_v(z)}{\partial z} = \frac{\partial X(z)}{\partial z} W_{cond,oda}$. The derivative of water loading with respect to z is obtained by (24). Water mass balance

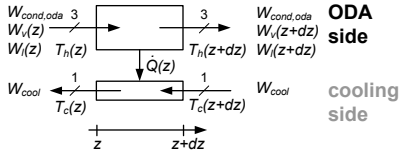

Fig. 2. Condenser differential model with mass and energy balance

across one cell leads to $\frac{\partial W_l(z)}{\partial z} = -\frac{\partial W_v(z)}{\partial z}$.

(24) $$\frac{\partial X(z)}{\partial z} = \frac{\partial X(T_h(z))}{\partial z} = \frac{\partial X(T_h)}{\partial T_h}\frac{\partial T_h(z)}{\partial z}$$

Equation (23) can be further reduced as it is dominated by enthalpy of evaporation h_0. Derivative of water loading with respect to temperature is approximated as the derivative at mean ODA temperature $T_{h,mean}$ in the condenser (25). Mean temperature is gained as the arithmetic mean of ODA in- and outlet temperature $T_{h,mean} = 1/2\,(T_{hout} + T_h)$. This leads to differential equation (26) on the ODA side of the condenser.

(25) $$\frac{\partial X}{\partial T} \approx \left.\frac{\partial X}{\partial T}\right|_{T_{h,mean}} = \left.\frac{dp_v^{sat}}{dT}\right|_{T_{h,mean}} \cdot \frac{p_c}{\left(p_c - p_v^{sat}(T_{h,mean})\right)^2}\frac{R_{oda}}{R_v}$$

(26) $$\left(h_0 W_{cond,oda}\left.\frac{\partial X}{\partial T}\right|_{T_{h,mean}}\right)\frac{\partial T_h}{\partial z} = C_h\frac{\partial T_h}{\partial z} = -U\left(T_h(z) - T_c(z)\right)$$

Model equations of the cooling side and equations of the ODA side are similar to model equations of a counter-flow heat exchanger with incompressible mass flows. Therefore, the effectiveness-NTU method [13] is applied. Condenser outflow temperature is governed as (27).

(27) $$T_{hout} = f(T_{hout}) = T_h - \varepsilon \cdot C_{\min}/C_h \cdot (T_h - T_c)$$

Effectiveness ε is obtained for a counter-flow heat exchanger (28) based on the effectiveness-NTU method [13] with $C_{min}=min(C_h,C_c)$, $C_{max}=max(C_h,C_c)$ and $NTU=UA/C_{min}$.

(28) $$\varepsilon = \frac{1-\exp\left(-NTU\left(1-C^*\right)\right)}{1-C^*\exp\left(-NTU\left(1-C^*\right)\right)} \text{ for } C^* = \frac{C_{\min}}{C_{\max}} \neq 1$$

$$\varepsilon = \frac{NTU}{1+NTU} \text{ for } C^* = 1$$

As the actual ODA outlet temperature T_{hout} is used to compute $\partial X / \partial T$ at mean temperature as well as C_h, it is obvious that T_{hout} is given by an implicit equation (27), which is solved for by the regula falsi method "Illinois Algorithm" [14]. As initial guess the interval with boundaries $[T_c\text{-}\varepsilon\ T_h]$ with $\varepsilon = 1K$ is taken. Outlet temperature T_{hout} is used to calculate the mass flow of vapor $W_{v,out} = X(T_{hout})W_{oda}$ and liquid leaving the condenser $W_{l,out} = W_{l,in}+W_{v,in}\text{-}W_{v,out}$ with the water loading calculated at outlet temperature T_{hout}. According to (22) an energy balance about the whole ODA side of the condenser delivers the heat flow transferred to the cooling side, which is taken to obtain the cooling outlet temperature T_{cout} by a static energy balance.

The condenser is considered to exhibit high cooling, which is modeled by a high heat transfer coefficient. ODA outlet temperature then is close to condenser cooling inlet temperature. As reported in [9], a value of $UA=600W/K$ is taken for the condenser model. Figure 3 shows stationary ODA-gas water loadings simulated for condenser cooling temperatures $T_{condin} = 5, 7.5, \ldots 20°C$ at a stack cooling inlet temperature of 55°C. Intuitively, water loading would decrease by lowering cooling temperature T_{condin} to let more vapor condense. Operating the condenser at $T_{condin} = 5°C$ would result in an ODA water loading X_{oda} of ca. 5g/kg. Water loadings of 5 to 15 g/kg lead to a 0.5-1.48% water mass flow of the total humid gas mass flow.

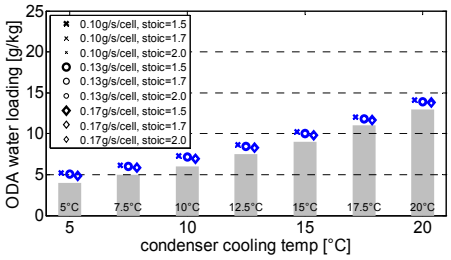

Fig. 4. Simulation: ODA water loading in exit manifold for condenser cooling inlet temperatures 5, 7.5…20°C, cell mass flows 0.10, 0.13, 0.17g/s/cell and stoichiometry 1.5, 1.7, 2.0, $T_{stackin}$ = 55°C

III. ODA Mass Flow Control

The MFC provides feed air and sets the air mass flow according to the reference $W_{mfc,ref}$, which is obtained by stoichiometry and stack current (29). Oxygen mass flow $W_{O2,react}$ (30) consumed by the chemical reaction reduces the feed air mass flow and leads to an ODA-gas mass flow.

(29) $$W_{mfc,ref} = \frac{I_{stack}}{4F} n_{cells} \lambda \left(M_{O2} + \frac{0.79}{0.21} M_{N2}\right)$$

(30) $$W_{O2react} = \frac{I_{stack}}{4F} n_{cells} M_{O2}$$

For inerting ODA oxygen content must be close to 10%. A stationary analysis [9] of the fuel cell system model shown in figure 4 reveals the dependency of oxygen content on stoichiometry. A value of $\lambda=1.72$ would lead to 10%. As the stoichiometry input for the system considered is quantized to values 1.60, 1.65, 1.70,… the controller model is derived for an operating point with $\lambda^* = 1.7$. The stack cooling inlet temperature is controlled for 55°C [8] and the condenser cooling inlet temperature for 5°C to achieve low ODA-gas water loading. Cooling controllers are assumed to work perfectly. When limiting stack current slope sufficiently, oxygen starvation, cathode flooding and hence serious dynamic voltage losses can be prevented. Although voltage dynamics of a PEM fuel cell are important, they can be neglected in the reduced order model as ODA-gas generation is independent of stack voltage. Further, thermal dynamics are slow and are neglected as well. Gas dynamics, however, are important. In [3] mass flows and pressures are modeled as static. So, nonlinear gas dynamics are approximated by first order time systems with time constant T_{MFC} and T_{FC} for the MFC and the fuel cell system. Model as well as mass flow controller uncertainties on feed air mass flow are accounted for by a disturbance z. Figure 5 shows the model with equations (31) and input $u=I_{stack}$ being the stack current, states x_1 and x_2 being the mass flows W_{mfc} provided by the MFC and ODA-gas W_{oda} leaving the fuel cell system. Model output y is ODA-gas mass flow. Measurement $W_{mfm}=y(t\text{-}T_d)$

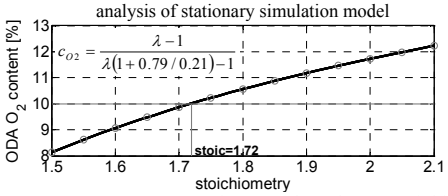

Fig. 3. ODA-gas oxygen concentration c_{O2} plotted over stoichiometry

is available with a time delay T_d. Assuming dry ODA-gas mass flow W_{oda} equalling W_{mfm} introduces a slight error of 0.5-1.48% for water loadings of 5-15g/kg motivating the approximation $W_{oda} = W_{mfm}$. Assuming a constant stoichiometry, the model is linear. This motivates to control for ODA-gas mass flow by a state feedback controller. As not all states are available through measurement, an observer estimates the states x_1, x_2 as well as disturbance z. For implementation the sampling time is T_s.

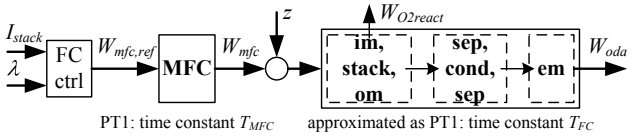

Fig. 5. Reduced order plant model for controller design

$$(31)\quad \underbrace{\begin{bmatrix}\dot{x}_1\\ \dot{x}_2\end{bmatrix}}_{\dot{x}} = \underbrace{\begin{bmatrix}-\frac{1}{T_{MFC}} & 0\\ \frac{1}{T_{FC}} & -\frac{1}{T_{FC}}\end{bmatrix}}_{A}\underbrace{\begin{bmatrix}x_1\\ x_2\end{bmatrix}}_{x} + \underbrace{\begin{bmatrix}\frac{n_{cells}\left(M_{O2}+\frac{0.79}{0.21}M_{N2}\right)}{T_{MFC}4F}\lambda^*\\ -\frac{n_{cells}}{T_{FC}4F}M_{O2}\end{bmatrix}}_{B}u + \underbrace{\begin{bmatrix}0\\ \frac{1}{T_{FC}}\end{bmatrix}}_{E}z$$

$$y = \begin{bmatrix}0 & 1\end{bmatrix}x = Cx$$

A. Observer and Predictor

State estimation takes place in two steps as proposed by [15] with a linear observer working in the past shifted by a time delay T_d to ensure time-synchronous u and y. Time delay T_d is compensated for by a predictor that takes the state estimate as initial condition to predict the actual state by applying the remaining plant input signal u.

1) Observer

A linear Luenberger Observer (32) estimates states x_1, x_2 and disturbance z. Gains L are obtained by pole placement.

$$(32)\quad \begin{bmatrix}\dot{\hat{x}}\\ \dot{\hat{z}}\end{bmatrix} = \begin{bmatrix}A & E\\ 0 & 0\end{bmatrix}\begin{bmatrix}\hat{x}\\ \hat{z}\end{bmatrix} + \begin{bmatrix}B\\ 0\end{bmatrix}u + L\left(y-\hat{y}\right) \text{and } \hat{y} = C\hat{x}$$

2) Predictor for $t - T_d \le \tau \le t$

The predictor model (33) is the system model extended by a disturbance, which stays constant throughout the prediction time horizon. The vector of initial conditions at time $\tau = t\text{-}T_d$ is the actual observer state vector estimated.

$$(33)\quad \begin{bmatrix}\dot{\hat{x}}(\tau)\\ \dot{\hat{z}}(\tau)\end{bmatrix} = \begin{bmatrix}A & E\\ 0 & 0\end{bmatrix}\begin{bmatrix}\hat{x}(\tau)\\ \hat{z}(\tau)\end{bmatrix} + \begin{bmatrix}B\\ 0\end{bmatrix}u(\tau) \text{ with } \begin{bmatrix}\hat{x}(\tau=t-T_d)\\ \hat{z}(\tau=t-T_d)\end{bmatrix} = \begin{bmatrix}\hat{x}(t-T_d)\\ \hat{z}(t-T_d)\end{bmatrix}$$

The system of differential equations is solved by a Runge-Kutta method of 4th order with time step less or equal to T_s. The system input is constantly $u(t\text{-}kT_s)$ for a sampling period $t\text{-}kT_s \le \tau \le t\text{-}(k\text{-}1)T_s$ with $k=(T_d/T_s), (T_d/T_s)\text{-}1, \ldots, 1$ provided that (T_d/T_s) is a natural number.

B. State Feedback Controller

To gain steady state accuracy of ODA-gas mass flow system (31) is extended by an additional state (34). A state feedback controller (35) is derived for the unconstrained extended system assuming availability of all states. Later, the controller receives the predictor states. Additional state e is the integral value of the sum of predictor output, reference value y_{ref} and discrepancy $T_R(u_R - u)$ between controller output u_R and limiter output u as a Classical Anti-windup approach [16] with time constant T_R to prevent integrator windup. Limiter output u (36) is governed using sampling time T_s. Stack current slope for rise and fall is limited to experimentally determined du_{max} to prevent the stack of flooding and oxygen starvation. Lower and upper bounds of u_{max} and u_{min} are set. Controller (35) is designed for the case $u_R = u$. Gain vector K is obtained by pole placement.

$$(34)\quad \begin{bmatrix}\dot{x}\\ \dot{\tilde{e}}\end{bmatrix} = \begin{bmatrix}A & 0\\ C & 0\end{bmatrix}\begin{bmatrix}\dot{x}\\ \tilde{e}\end{bmatrix} + \begin{bmatrix}B\\ 0\end{bmatrix}u + \begin{bmatrix}0\\ -1\end{bmatrix}y_{ref} \text{ and } y = C\hat{x}$$

$$(35)\quad u_R = -K\begin{bmatrix}\hat{x} & e\end{bmatrix}^T \text{ with } e = \int C\hat{x} - y_{ref} + T_R\left(u_R - u\right)dt$$

$$(36)\quad u_R^*(t) = \begin{cases} u(t-T_s) + du_{\max}T_s & , u_R(t) - u(t-T_s) > +du_{\max}T_s \\ u(t-T_s) - du_{\max}T_s & , u_R(t) - u(t-T_s) < -du_{\max}T_s \\ u_R(t) & , otherwise \end{cases}$$

$$u(t) = \begin{cases} u_{\max} & , u_R^*(t) > u_{\max} \\ u_{\min} & , u_R^*(t) < u_{\min} \\ u_R^*(t) & , otherwise \end{cases}$$

Inaccuracies in the MFC flow control lead to an increase of the cathode feed air mass flow compared to the reference value resulting in an increase of ODA-gas O_2 content. This can be corrected by decreasing stoichiometry. An underlying lambda feedback for integral control of stoichiometry [17] to gain a 10% oxygen content, however, would lead to oscillations due to the quantized input signal. Experiments revealed, that a 10% ODA-gas O_2 concentration is gained for stoichiometry 1.6. Therefore, stoichiometry is reduced manually from 1.7 to 1.6. The effect of providing too much cathode feed air in the nonlinear simulation model is captured by setting a 107% delivery of mass flow $W_{mfc,ref}$. This mimics a disturbance on air mass flow. The plant model with time delay on mass flow measurement, the state feedback controller, observer and predictor are shown in figure 6. The controller is run with sampling time T_s.

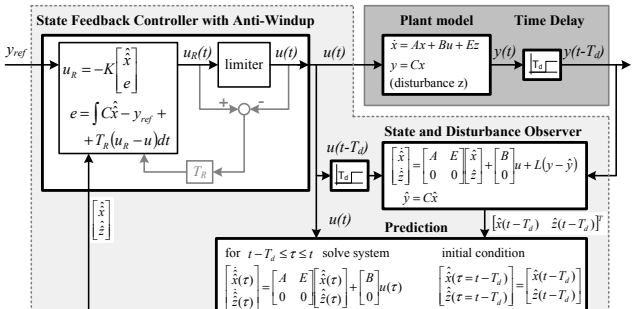

Fig. 6. Schematic of the ODA state feedback controller with Anti-Windup circuit, observer, predictor and plant model with time delay

IV. Simulation and Experimental Results

The state feedback controller, observer for state estimation and predictor for time delay compensation were run on the nonlinear fuel cell system simulation model in Matlab/Simulink® and were applied to the real plant. ODA-gas reference mass flows are 0.1 and 0.17g/s/cell. Stack and condenser inlet cooling temperatures are controlled for 55°C and 5°C, respectively. Stoichiometry was set constant to a value of 1.6. Simulation and experimental results are shown

in figure 7. In the simulation as well as in the experimental run the controller adjusts stack current such that the ODA-gas reference mass flow is reached quickly. The offset in stack current is due to differing disturbance mass flows in simulation and experiment. Oxygen concentration is close to 10% and a low water loading is gained with simulation and experimental values being very close at circa 5g/kg. The controller performs very well.

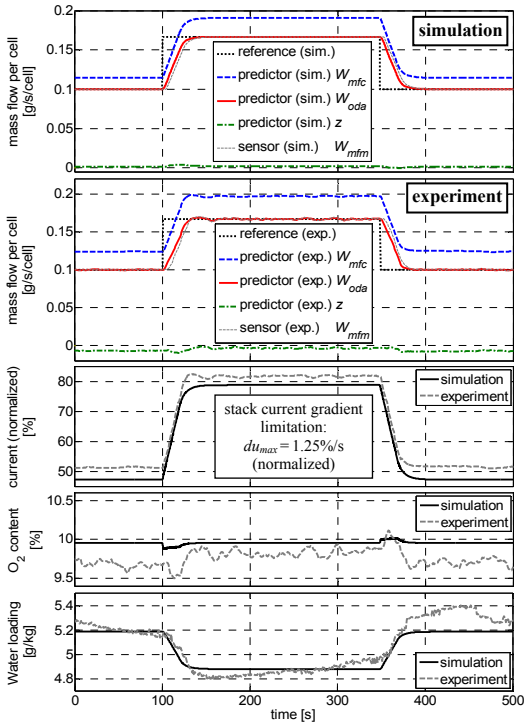

Fig. 7. Simulation end experimental results for an ODA-gas mass flow reference $W_{oda,ref}$ of 0.1 and 0.17g/s/cell: predictor outputs and ODA-gas mass flow signal (top); stack current as input signal normalized to u_{max} (center); ODA-gas oxygen content and water loading (bottom)

V. Conclusion

For a PEM fuel cell system consisting of the stack, stack cooling system and cathode exhaust gas dehumidifying system a control strategy is developed to control for the cathode exhaust gas mass flow. A linear reduced order model is used for state feedback controller design. System states and disturbances are estimated by a linear observer and a predictor is used to compensate for a significant time delay occurring due to gas transport. The control strategy is successfully applied to the nonlinear simulation model and the real plant and results of both are shown.

References

[1] E. Vredenborg, H. Lüdders and F. Thielecke, "Methodology for Sizing and Simulation of complex Fuel Cell Systems" orig.(german) "Methodik zur Auslegung und Simulation komplexer Brennstoffzellensysteme", *DLRK 2010*, Hamburg, 2010.

[2] J. Bleil, "Fuel Cells for onboard Power Supply of Aircraft", orig. (german) "Brennstoffzellen zur Bordstromversorgung von Flugzeugen", *HZwei-Das Magazin für Wasserstoff und Brennstoffzellen*, 04/2007

[3] J. Niemeyer, *Model Predictive Control of a PEM-Fuel Cell System*, orig. (german) Modellprädiktive Regelung eines PEM-Brennstoffzellensystems, Schriften des Instituts für Regelungs- und Steuerungssysteme, Universität Karlsruhe, Band 05, 2009

[4] J. T. Pukrushpan, A. G. Stefanopoulou and H. Peng, *Control of Fuel Cell Power Systems.* London: Springer-Verlag, 2004.

[5] A. Y. Karnik, J. Sun, A. G. Stefanopoulou and J. H. Buckland, "Humidity and Pressure Regulation in a PEM Fuel Cell Using a Gain-Scheduled Static Feedback Controller", *IEEE Transactions on Control Systems Technology*, vol.17, No.2, pp. 283-297, 2009

[6] R. Borup et al., "Scientific Aspects of Polymer Electrolyte Fuel Cell Durability and Degradation", *Chem. Rev.*, vol. 107, pp. 3904-3951, 2007

[7] D. A. McKay, W. T. Ott and A. G. Stefanopoulou, "Modeling, Parameter Identification and Validation of Reactant and Water Dynamic for a Fuel Cell Stack", *Proceedings of the 2005 ASME International Mechanical Engineering Congress & Exposition*, 2005

[8] M. Schultze, M. Kirsten, S. Helmker and J. Horn, "Modeling and Simulation of a Coupled Double-Loop-Cooling System for PEM-Fuel Cell Stack Cooling", *2012 UKACC International Conference on Control*, pp. 857-863, 2012

[9] M. Schultze and J. Horn, "Optimization Approach for Cathode Exhaust Gas Conditioning of a Multifunctional PEM Fuel Cell System for the Application in Aircraft", *DLRK* 2012, Berlin, 2012

[10] H. D. Baehr and S. Kabelac, *Thermodynamics*, orig. (german) Thermodynamik, Berlin: Springer-Verlag, 2006

[11] J. C. Amphlett, R. M. Baumert, R. F. Mann, B. A. Peppley and P. R. Roberge, "Performance Modeling of the Ballard Mark IV Solid Polymer Electrolyte Fuel Cell", *J. Electrochem. Soc.*, vol. 142, pp. 1-8, 1995

[12] R. O'Hayre, S.-W. Cha, W. Colella and F. B. Prinz, *Fuel Cell Fundamentals*. Hoboken, NJ: John Wiley & Sons, 2009.

[13] R. K. Shah and D. P. Sekulic, *Fundamentals of Heat Exchanger Design*, Hoboken, NJ: John Wiley & Sons, 2003

[14] J.A. Ford, "Improved Algorithms of Illinois-type for the Numerical Solution of Nonlinear Equations", *Technical Report CSM-257*. University of Essex Press, 1995

[15] J. Birk, „State Estimation for Nonlinear Processes with Discrete-Time and Time-Delayed Measurements" orig.(german) "Zustandsschätzung für nichtlineare Prozesse mit zeitdiskreten und totzeitbehafteten Messgrößen", *at - Automatisierungstechnik* 48, 2000

[16] C. Edwards and I. Postlethwaite, "Anti-Windup and Bumpless Transfer Schemes", *UKACC International Conference on Control '96*, vol. 1, pp. 394-399, 1996

[17] M. Schultze and J. Horn, "Control strategy for mass flow and oxygen concentration of PEM Fuel Cell exhaust gas" orig. (german) "Regelungsstrategie für Massenstrom und Sauerstoffkonzentration für sauerstoffarmes Abgas von PEM-Brennstoffzellensystemen", GMA-FA 1.30, Anif/Salzburg, 2012

TABLE I. Fuel Cell System Model Parameters

Parameter	Description
M_{O2}, M_{N2}	molar masses of oxygen (O_2) and nitrogen (N_2)
R_v, R_{oda}, R_{O2}, R_{N2}	gas constants of water vapor, ODA-gas, oxygen and nitrogen
c_{air}, c_{oda}, c_l, c_v, c_{cool}, C_{stack}	specific heat capacities of air, ODA-gas, water, vapor, coolant in inner loop, stack heat capacity
h_o	enthalpy of evaporation
c_{sep1}, c_{sep2}, c_{cond}	mass flow constants for turbulent flow
F	Faraday's constant
n_{cells}, A_{sfc}, d_m	number of cells in the stack, active surface area, membrane thickness
V_i	volume
W_i, m_i	mass flow, mass
p_i	pressure
X_i	water loading
T_i	temperature
T_{MFC}, T_{FC}	time constants
T_s, T_d, T_R	sampling time, time delay, Anti-Windup parameter
ζ_i, b_i	stack voltage model parameters
I_{stack}, λ	stack current, stoichiometry